QC-06-002 (RP-1311)

Thermal Resistance of a Window with an Enclosed Venetian Blind: Guarded Heater Plate Measurements

Ned Y.T. Huang

John L. Wright, PhD, PEng
Member ASHRAE

Michael R. Collins, PhD
Associate Member ASHRAE

ABSTRACT

Window solar gain is known to have a strong influence on building energy consumption and peak cooling load. Venetian blinds are routinely used to control solar gain. Software based on one-dimensional models is available to accurately predict the thermal performance of glazing systems, but the development of models for windows with shading devices is at a very early stage. A guarded heater plate apparatus has been used to measure center-glass heat transfer rates through a double-glazed window with a venetian blind in the glazing cavity. Variables examined include pane spacing, temperature difference, slat angle, and the presence of a low-emissivity coating. Results were compared with earlier measurements. The data collected provide direct guidance in the development of models to predict U-factor and solar gain for this type of glazing/shading system, leading to a more structured and quantitative design procedure.

INTRODUCTION

Window area and its associated design, distribution, orientation, etc., affect solar gain and heat losses of a building. Proper fenestration design can greatly reduce unwanted energy gains/losses and can help maintain a comfortable indoor space. Solar gain is of particular importance because of both its magnitude and variability. Shading devices such as venetian blinds, roller blinds, and drapes are frequently used to control solar gain.

One-dimensional models have been developed (e.g., Finlayson et al. [1993], Hollands et al. [2001], Hollands and Wright [1983], Wright [1980, 1998], and Rubin [1982]) and are known to accurately predict the thermal performance of glazing systems (e.g., Carpenter [1992] and Wright and Sullivan [1987]). Software based on these models is widely used for design, code compliance, and rating. In contrast, the development of models for windows with shading devices is at a very early stage.

A set of experiments was undertaken to measure the center-glass thermal resistance of a doubled-glazed window with an enclosed (i.e., in the glazing cavity) venetian blind. The venetian blind was placed in the most common configuration, a vertical layer composed of horizontal slats. A cross section of this arrangement is shown in Figure 1. The geometry is described by the slat width w, distance between slats s, slat angle ϕ, slat curvature r_c, and pane spacing L. The heat flux, driven by temperature difference across the assembly, is q".

Heat transfer measurements were done using a guarded heater plate (GHP) apparatus. Described briefly, the GHP apparatus consists of two isothermal plates. Once a test sample is installed between these plates, it is possible to measure the heat flux through the sample, driven by the temperature difference between the plates. The current research is an extension of work by Garnet (Garnet et al. 1995; Garnet 1999), completed with the same apparatus. The most noteworthy extension is that a low-emissivity (low-e) coating has been used in some of the new test samples.

The GHP measurements represent a key step toward the development of models that can include the influence of enclosed venetian blinds in otherwise conventional glazing systems. It is clear that the measured thermal resistance values can be directly applied to the calculation of nighttime U-factors. Several simplified models have already been devised and compared to the GHP measurements of Garnet (Yahoda 2002; Yahoda and Wright 2004a, 2004b) with

Ned Y.T. Huang is a mechanical research and development engineer with Atomic Energy of Canada Limited, Chalk River Laboratories, Chalk River, Ontario, Canada. **John L. Wright** and **Michael R. Collins** are professors in the Department of Mechanical Engineering, University of Waterloo, Waterloo, Ontario, Canada.

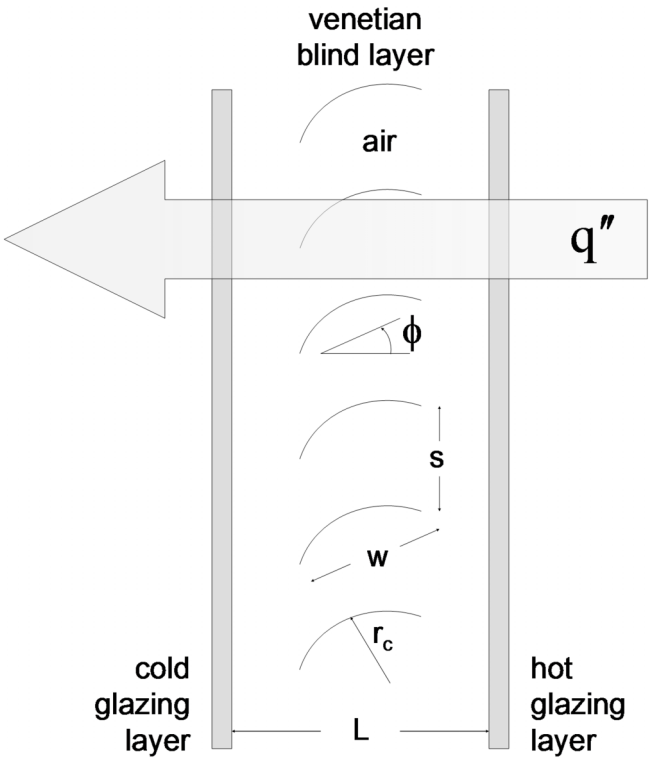

Figure 1 *Schematic of double-glazing with an enclosed venetian blind.*

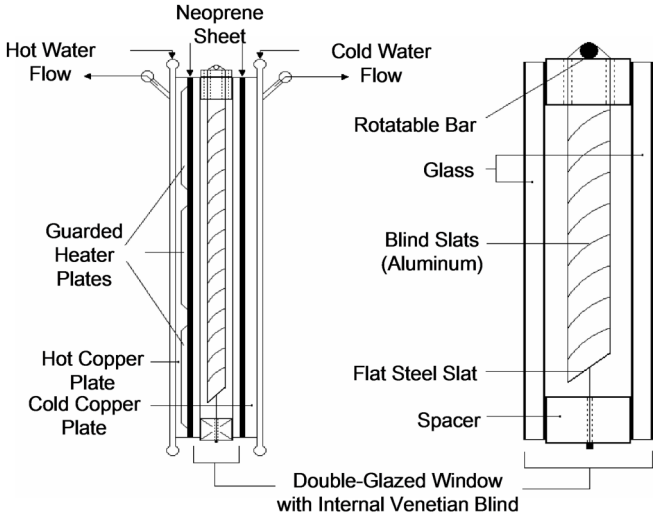

Figure 2 *Copper plates and double-glazed window with an enclosed venetian blind.*

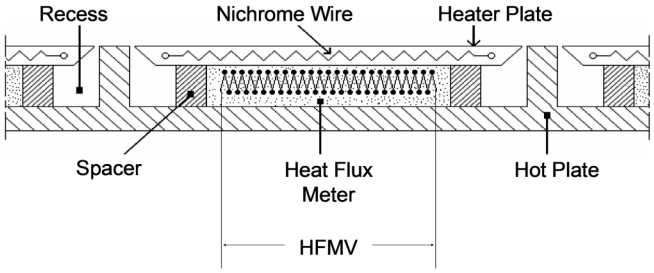

Figure 3 *Detail of heater plate and heat flux meter.*

moderate success. In addition, the same measurements, although done in the absence of solar radiation, can be used to obtain daytime U-factors and solar heat gain coefficients (SHGCs). The planned course of action is to augment the GHP measurements with computational fluid dynamics (CFD) calculations. The CFD models, validated with GHP measurements, can be extended to account for the presence of solar radiation. In particular, it will be possible to obtain the inward-flowing fractions of absorbed solar radiation. The more detailed models are also expected to lead to simplified models that apply to the full range of sunlit conditions. Research is well under way in this effort (Tasnim 2005).

THE GUARDED HEATER PLATE APPARATUS

The GHP apparatus has been used in many heat transfer experiments. It was designed to measure convective heat transfer across air-filled rectangular cavities (e.g., ElSherbiny [1980] and ElSherbiny et al. [1982]) but was more recently adapted to measure heat transfer through samples that include solid components (e.g., Wright and Sullivan [1987, 1988, 1989, 1995] and Hum et al. [2004]).

The apparatus consists mainly of two copper plates. Figure 2 shows a schematic of the apparatus with a test sample in place. Each copper plate is 12.7 mm (0.5 in.) thick with face dimensions of 635 × 635 mm (25 × 25 in.). The desired hot and cold plate temperatures are maintained by circulating a water/glycol mixture from constant temperature baths to copper tubes soldered to the back of each plate. When a glazing assembly is tested, as in this study, thin neoprene sheets (approximately 1.6 mm [1/16 in.] thick) are placed between the glass and copper surfaces to eliminate contact resistance.

Three recesses in the hot copper plate contain three guarded heater plates. The detail of one heater plate is shown in Figure 3. Each heater plate is 3.1 mm (0.122 in.) thick with face dimensions of 200 × 200 mm (7.874 × 7.874 in.). A heat flux meter is sandwiched between the heater plate and the main hot copper plate. The heat flux meters are flexible, rubbery disks that each contain a thermopile with a large number of junctions (approximately 800 junctions). Each heat flux meter senses the temperature difference between a heater plate and the hot copper plate and produces an output signal, the heat flux meter voltage (HFMV). Measurements are completed by adjusting the electrical power supplied to the nichrome wire in the heater plate until there is no temperature difference between the heater plate and the hot copper plate. This condition of zero temperature difference implies that there is no heat transfer between the heater plate and the hot plate. Therefore, the rate at which electrical energy is supplied

must be equal to the rate of heat transfer from the exposed face of the heater plate.

The GHP apparatus is a very accurate device because (1) the electrical power supplied to the heater plates can be determined with voltage and current measurements that entail no appreciable uncertainty and (2) the heat flux meter is a passive device that reliably detects the desired null condition without offset. The GHP apparatus requires no calibration or comparison with a calibration standard.

THE TEST SAMPLES

Test samples were built by using machined acrylic edge-spacers to separate two sheets of glass. The top and bottom spacers were modified to hold the venetian blind at the center of the glazing cavity. A false face was added to one of the side spacers to provide a small cavity for desiccant. Three sets of spacers produced pane spacings of L = 17.78 mm (0.7 in.), L = 25.40 mm (1.0 in.), and L = 40.01 mm (1.575 in.). The face dimensions of the samples were the same as the copper plates: 635 × 635 mm. Two samples were built for each of the three pane spacings. First, the "clear/clear" sample consists of two layers of 3-mm-thick clear glass. Second, as in the "clear/clear" sample, the "clear/low-e" sample also has two layers of 3 mm clear glass, but a low-e coating was present on the cavity side of the hot glazing. The hemispheric emissivity of uncoated glass is known to be $\varepsilon_{gl} = 0.84$. The normal hemispheric longwave reflectivity of the low-e coating was measured using a Gier-Dunkle DB-100 infrared reflectometer. The result was converted to hemispheric emissivity (Rubin et al. 1987) giving $\varepsilon_{le} = 0.164$.

Garnet (1999) also used spacings of 17.78 mm (0.7 in.), 25.40 mm (1.0 in.), plus an intermediate spacing of 20.32 mm (0.8 in.). His venetian blind and spacer assemblies for the first two cavity widths were carried over to this research. None of Garnet's test samples included a low-e coating.

The smallest pane spacing, L = 17.78 mm, was chosen because this dimension represents a tight fit between the venetian blind and the walls of the glazing cavity when the slats are fully open, $\phi = 0$. The next spacing used in this study, L = 25.40 mm, gives information about the influence of pane spacing. Both of these smaller pane spacings could realistically be used in a consumer product. In contrast, the largest pane spacing, $L \approx 40$ mm, is not seen as a popular, or even likely, design option. This large spacing was studied in the hope of obtaining rough information about the smallest spacing at which ϕ and/or L have little or no effect on q''.

The same venetian blind was used in each test sample. It is a commercial product with painted aluminum slats (w = 14.79 mm, s = 11.84 mm, $r_c/w \approx 2.0$). The thickness of the slat material was 0.20 mm (0.008 in.) as tested or 0.18 mm (0.007 in.) with the paint removed. The composition of the aluminum, undoubtedly an alloy, is not known, so its thermal conductivity is also unknown—except to say that it will be high. The hemispheric emissivity of the painted slat surfaces, again obtained using the Gier-Dunkel DB-100 instrument, is $\varepsilon_{slat} = 0.792$.

The edges of the test samples, which would otherwise be exposed to the laboratory environment, were insulated.

MEASUREMENT DETAILS

Experiments were completed with two different temperature-difference settings. The thermostat setting of the warm, constant temperature bath was 30°C in all cases. The cold bath was set to either 20°C (ΔT_{bath} = 10°C) or 10°C (ΔT_{bath} = 20°C). The controllers are able to maintain the bath temperatures to within 0.1°C. The circulating fluid changes temperature modestly as it passes through the apparatus, so the measured plate-to-plate temperature difference, ΔT_{pp}, is always slightly less than ΔT_{bath}.

The slat angle was adjusted over the range $-75° \le \phi \le 75°$, the maximum range allowed by the support-string mechanism. Note that, with reference to Figure 1, a positive slat angle, $\phi > 0$, indicates that the tip of the blind next to the hot glazing is inclined upward.

All three heat flux meters were balanced in order to obtain the desired isothermal boundary condition, but only the heat flux measured at the center guarded heater plate is presented. This value is known to be a representative measure of the center-glass heat flux because of insight gained from previous research, including guarded heater plate measurements and the corresponding simulation results (e.g., Wright and Sullivan [1994, 1995]).

DETERMINING CENTER-GLASS U-FACTOR

The total thermal resistance of the test assembly, including the two neoprene mats and the double-glazed test sample, was determined from the plate-to-plate temperature difference, ΔT_{pp}, and the measured heat flux, q'':

$$R_{tot} = \frac{\Delta T_{pp}}{q''} \tag{1}$$

The total resistance R_{tot} includes the glass-to-glass thermal resistance R_{gg} plus the resistance of two neoprene sheets, $2R_n$:

$$R_{tot} = R_{gg} + 2R_n \tag{2}$$

The thermal resistance of the neoprene sheets was measured using the GHP apparatus, giving: $2R_n = 0.01$ m^2 K/W.

The indoor-outdoor thermal resistance of a window includes convective and radiative heat transfer between the exposed surfaces and the environment. The corresponding thermal resistance components were represented by the outdoor film coefficient h_o and indoor film coefficient h_i. Therefore, the center-glass U-factor, U_{cg}, was obtained using

$$U_{cg} = \frac{1}{(1/h_o) + R_{gg} + (1/h_i)} . \tag{3}$$

The film coefficients h_o and h_i vary with environmental conditions. Garnet (1999) chose to use fixed values of $h_i = 8.0$ W/m^{2}K and $h_o = 23.0$ W/m^{2}K. The same values were used in the current study for ease of comparison.

ESTIMATED UNCERTAINTY

Propagation of Uncertainty

Uncertainty associated with GHP measurements was tracked using the conventional root-mean-square calculation (e.g., Moffat [1985]). Consider a result, R, that is obtained as a function of a set of measurements, x_i. The uncertainty in R, δR, propagating from the uncertainty in each x_i, δx_i, , is

$$\delta R = \left\{ \sum_i \left(\delta x_i \frac{\partial R}{\partial x_i} \right)^2 \right\}^{\frac{1}{2}}. \quad (4)$$

Applying Equation 4 to the GHP measurements of the various test samples, the result of interest is U_{cg} and the measurements used to obtain U_{cg}, the x_i, are ΔT_{pp}, q'', and $2R_n$.

Uncertainty in ΔT_{pp}

Prior to the current research, a new thermopile, consisting of six T-type thermocouples in each plate, was installed in the GHP apparatus. Rasiah (2003) performed a calibration and uncertainty analysis using the procedures of Wheeler and Ganji (1996). Rasiah estimated an uncertainty in ΔT_{pp} of $\delta\Delta T_{pp} = \pm 0.06$°C. This very low uncertainty relies on the use of a correction obtained by experiment. Without this empirical correction, an uncertainty of $\delta\Delta T_{pp} = \pm 0.1$°C was estimated. These estimates of $\delta\Delta T_{pp}$ include a contribution associated with the ITS-90 thermocouple inverse polynomials (e.g., Omega [2004]). In the present study, the error caused by the inverse polynomial was avoided by using only the direct polynomial in combination with a root-finding procedure. This refinement, in combination with the empirical correction, reduces the uncertainty to $\delta\Delta T_{pp} = \pm 0.05$°C.

Values of $\delta\Delta T_{pp}$ reported in this paper were calculated without applying the empirical correction of Rasiah. Therefore, a value of $\delta\Delta T_{pp} = \pm 0.1$°C was used in subsequent calculations and this value is considered conservative because the reverse polynomial was not used.

Uncertainty in q''

The cyclic operation of the thermostats in the constant temperature baths can be detected as a cyclic swing in HFMV. Detail is provided by Wright and Sullivan (1988). The resulting uncertainty in HFMV is estimated to be δHFMV = ±0.1 mV. This translates into an uncertainty in measured heat flux that can be quantified by examining the relation between HFMV and the rate at which electrical power is supplied to the heater plate. A value of $\delta q'' = 0.3$ W/m^2 was found to apply to all experiments undertaken with test samples in place. In the calibration of the two neoprene sheets, the uncertainty in HFMV corresponds to $\delta q'' = 0.8$ W/m^2.

Uncertainty in $2R_n$

The thermal resistance $2R_n$ was measured by installing only the two neoprene sheets in the GHP apparatus. In this case Equation 1 can be applied with $2R_n$ replacing R_{tot} and the only measurements, x_i, contributing to the result are ΔT_{pp} and q''. The combination of Equations 1 and 4 yields Equation 5, which when applied gives $\delta 2R_n = \pm 0.04\ (2R_n)$ (i.e., 4% uncertainty).

$$\frac{\delta(2R_n)}{2R_n} = \left[\left(\frac{\delta(\Delta T_{pp})}{\Delta T_{pp}} \right)^2 + \left(\frac{\delta q''}{q''} \right)^2 \right]^{\frac{1}{2}} \quad (5)$$

In this case the possible uncertainty in measured heat flux was insignificant compared to the uncertainty in ΔT_{pp}.

Uncertainty in U-Factor

The uncertainty attached to the measurements of U_{cg} was also estimated. Applying Equation 4 to the combination of Equations 1, 2, and 3 yields

$$\frac{\delta U_{cg}}{U_{cg}} = U_{cg} R_{tot} \left[\left(\frac{\delta(\Delta T_{pp})}{\Delta T_{pp}} \right)^2 + \left(\frac{\delta q''}{q''} \right)^2 + \left(\frac{2R_n}{R_{tot}} \frac{\delta(2R_n)}{2R_n} \right)^2 \right]^{\frac{1}{2}}. \quad (6)$$

Depending on the specific test sample and setup, the uncertainty would decrease if, by testing at a higher ΔT_{pp}, the level of heat flux were raised. The nominal ΔT_{pp} was either 10°C or 20°C, and q'' ranged from 21 to 113 W/m^2. The uncertainty in HFMV of ±0.1 mV corresponds to values of $\delta q''$, ranging from about 0.27 W/m^2 for the $L = 17.78$ mm spacing to about 0.29 W/m^2 for the $L = 40$ mm spacing. It was found that the uncertainty in measured U-factor ranged from 0.3% to 1.3%. Clearly, the GHP apparatus provides a very accurate measurement. It is likely that similar uncertainty arises simply from details in the construction of the test samples and/or the visual measurement of the slat angle.

RESULTS AND DISCUSSION

Figure 4 shows a comparison of the measurements made by Garnet (1999) and a subset of the results from the current research. Values of U_{cg} are shown as a function of slat angle for $L = 17.78$ mm and $L = 25.4$ mm. The data shown in Figure 4 pertain to $\Delta T_{bath} = 20$°C. No low-e coating was present. The results of the two data sets match well for $\phi < 0$ (within 2.5%) but differ more for $\phi > 0$ (up to about 8%). It is interesting to note that there is an irregular "bump" at $\phi \approx -60°$ for the $L = 25.4$ mm spacing. It had been thought some of the measurements of Garnet should be discarded as outliers, but the irregularity has been reproduced.

Very recently Avedissian and Naylor (2005) compared a two-dimensional numerical model to the current measured results for the $L = 25.4$ mm spacing. They reported a maximum

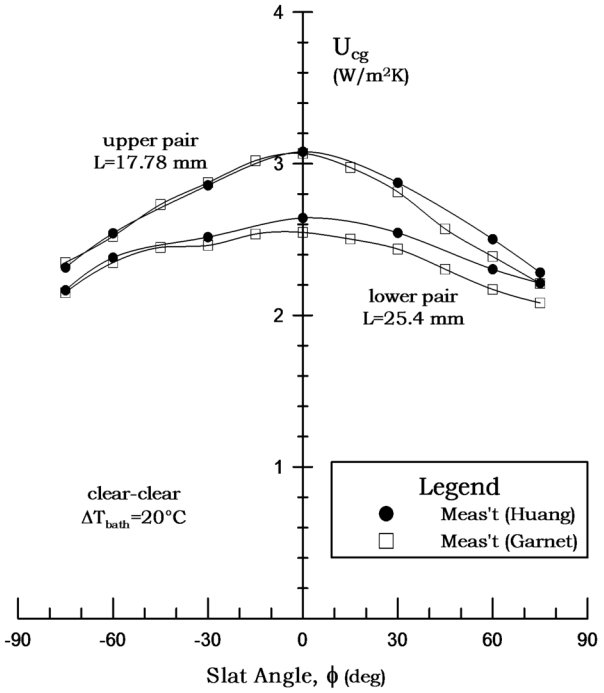

Figure 4 *Comparison of U-factor measurements with Garnet (1999).*

difference of about 1% for $\phi > 0$ and about 4% for $\phi < 0$. In this case the reason for the difference was the inability of the numerical model to reproduce the "bump" at $\phi \approx -60°$. Further research will be required to determine the cause of the bump.

Measured U-Factors

Tables 1 to 3 show all measured U_{cg} values (Huang 2005). In these tables, "clear" represents cases without low-e coating. The label "low-e" indicates that a low-e coating was present.

The measured U-factors listed in Tables 1 to 3 are also plotted as U_{cg} versus ϕ in Figures 5 to 7. In each plot, as indicated by the legend, the upper curves pertain to test samples built with no low-e coating. The two sets of data presented for each test sample correspond to the two temperature difference settings used. Figure 8 shows a summary plot of all measured U_{cg}.

Effect of Slat Angle, ϕ

The measurements show, for all test samples but one, that U_{cg} is maximum when the venetian blind is fully open, $\phi = 0$, and decreases as the blind is closed in either direction. As the blind is closed, radiant exchange is reduced simply because the slats block more longwave radiation. In other words, the shielding created by the venetian blind contributes to the bell-shaped curvature in the U_{cg} versus ϕ plots. This was demonstrated by Yahoda and Wright (2004b). Convective heat transfer is also affected by ϕ as the altered slat geometry causes the fill gas to move differently. Little can be said about the influence of ϕ on either individual mode of heat transfer until more detail is known about the convective mode of heat transfer.

Table 1. Measured U_{cg} (W/m² K), L = 17.78 mm (0.7 in.)

Slat angle, ϕ (deg)	Clear ΔT_{bath} = 20°C	Clear ΔT_{bath} = 10°C	Low-e ΔT_{bath} = 20°C	Low-e ΔT_{bath} = 10°C
–75	2.32	2.37	1.87	1.93
–60	2.54	2.53	2.02	2.08
–30	2.86	2.92	2.38	2.40
0	3.08	3.10	2.65	2.64
30	2.87	2.91	2.38	2.45
60	2.50	2.56	2.00	2.03
75	2.28	2.32	1.84	1.85

Table 2. Measured U_{cg} (W/m²K), L = 25.40 mm (1.0 in.)

Slat angle, ϕ (deg)	Clear ΔT_{bath} = 20°C	Clear ΔT_{bath} = 10°C	Low-e ΔT_{bath} = 20°C	Low-e ΔT_{bath} = 10°C
–75	2.17	2.17	1.65	1.62
–60	2.38	2.29	1.84	1.73
–30	2.52	2.57	1.87	1.92
0	2.64	2.68	1.94	1.97
30	2.54	2.60	1.85	1.88
60	2.30	2.36	1.68	1.69
75	2.21	2.20	1.63	1.62

Table 3. Measured U_{cg} (W/m² K), L = 40.01 mm (1.575 in.)

Slat angle, ϕ (deg)	Clear ΔT_{bath} = 20°C	Clear ΔT_{bath} = 10°C	Low-e ΔT_{bath} = 20°C	Low-e ΔT_{bath} = 10°C
–75	2.14	2.06	1.78	1.63
–60	2.27	2.25	1.74	1.63
–30	2.43	2.40	1.73	1.63
0	2.49	2.45	1.76	1.61
30	2.47	2.41	1.81	1.64
60	2.35	2.28	1.82	1.68
75	2.20	2.15	1.78	1.65

The direction of slat closure does not have a significant impact on U-factor. Comparing U_{cg} at ϕ versus $-\phi$ shows that, with one exception, the measured U_{cg} differ by less than 5%. The larger discrepancies are associated with the "bump" discussed earlier.

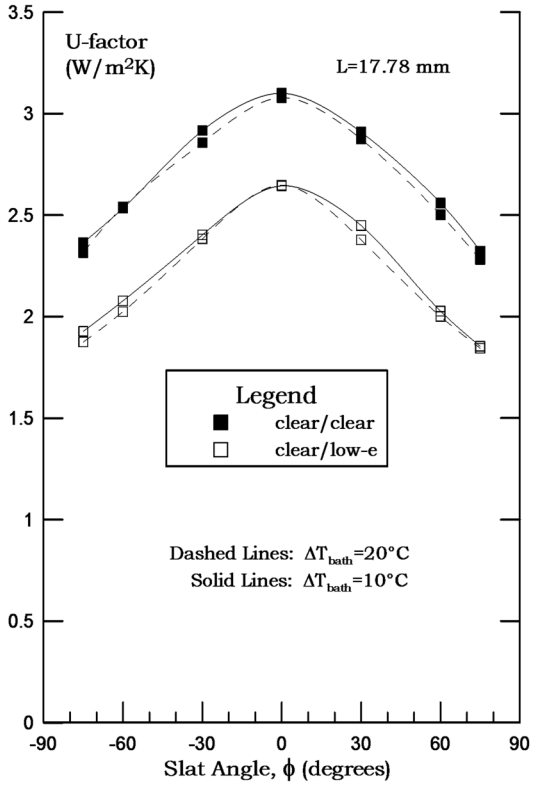

Figure 5 *Measured U-factor as a function of ϕ for L = 17.78 mm (0.7 in.).*

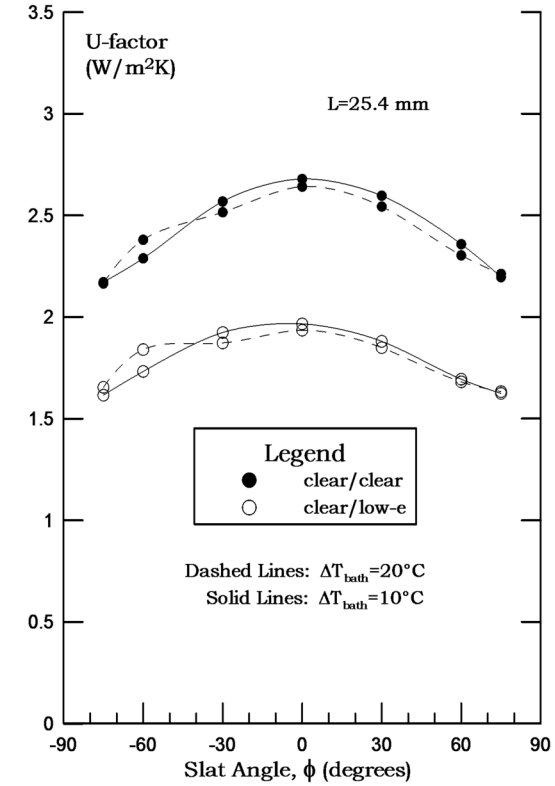

Figure 6 *Measured U-factor as a function of ϕ for L = 25.40 mm (1.0 in.).*

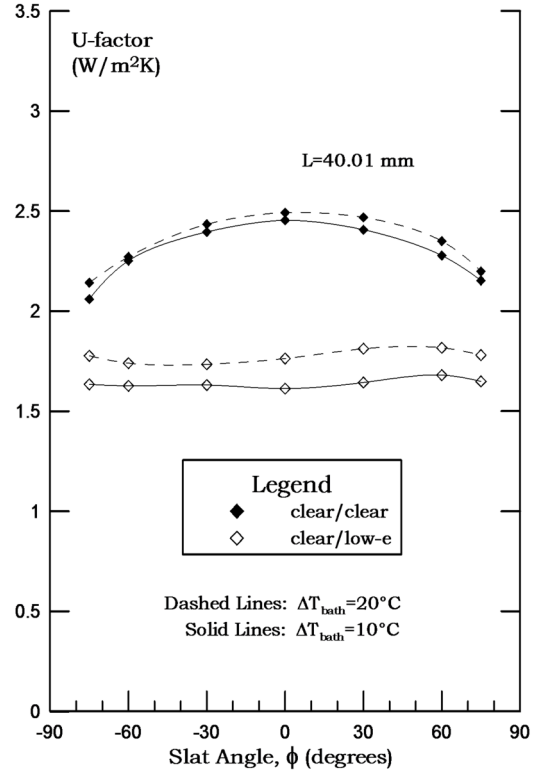

Figure 7 *Measured U-factor as a function of ϕ for L = 40.01 mm (1.575 in.).*

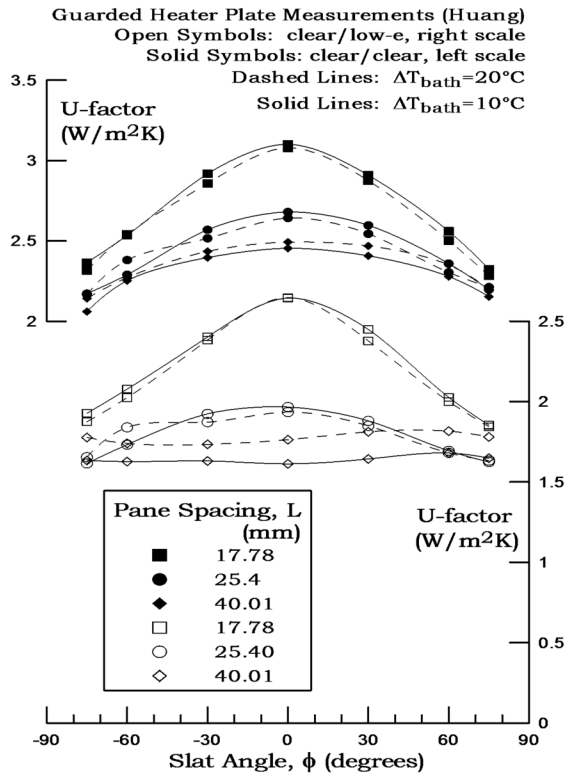

Figure 8 *Measured U-factor as a function of ϕ for all cases.*

Effect of Low-e Coating

The addition of a low-e coating resulted in a downward shift of U-factor in all cases and the improvement in window performance is appreciable. The U-factors were lowered by 15% to 35%.

The one exception, where U_{cg} was not found to be maximum at $\phi = 0$, was the test sample with low-e coating and the largest pane spacing, $L = 40.01$ mm. See the lower set of curves in Figure 7. In this case ϕ had little influence at all and this might have been expected because (a) the slat geometry will have little influence on the convective heat transfer in a cavity of large pane spacing and (b) the influence of longwave shielding will be reduced because of the low-e coating. The influence of shielding can be seen by comparing the upper curves to the lower curves in Figure 7. If a low-e coating is present the curves are relatively flat, but without a low-e coating the curvature associated with shielding is apparent.

Effect of Temperature Difference

The measurements plotted in Figure 8 show, for all test samples but one, that the influence of ΔT_{bath} can be ignored—particularly for engineering purposes. The choice of temperature difference did not change U_{cg} significantly (0% to 5%) when samples with $L = 17.78$ mm or $L = 25.4$ mm were tested.

Figure 6 shows two "bumps" near $\phi = -60°$. This irregularity was only found in samples constructed with $L = 25.4$ mm and tested at the higher temperature difference. It is certain that this variation in U_{cg}, an excursion of about 7%, is caused by a change in the convective flow induced only at a particular combination of T, L, and ϕ because no similar behavior would be expected with regard to the radiant heat transfer.

The influence of temperature difference arose when samples were tested with the largest pane spacing, $L = 40.01$ mm (see Figures 7 and 8). Although the effect of temperature difference is not readily apparent when no low-e coating is present, the effect of ΔT was clearly detected when a low-e coating was included in the test sample. Consider the latter case. With a low-e coating present, the influence of convection is not overshadowed by the radiant exchange and the changes in convective flow (possibly including formation of cells, unsteady flow, and turbulence) expected at larger spacing and larger temperature difference (i.e., larger values of Rayleigh number) influence U_{cg}. Lower temperature difference was found to result in lower U-factor, this despite the increase in radiant heat transfer (about 5%) expected to accompany the increase in mean temperature (about 5 K in 300 K) within the cavity. See Hollands et al. (2001) for commentary concerning the effect of mean temperature.

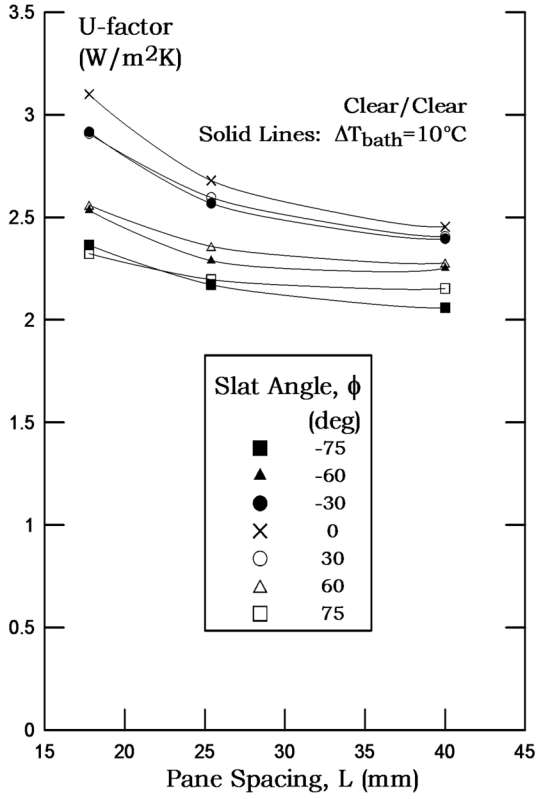

Figure 9 *Measured* U_{cg} *as a function of* L *for various slat angles,* ϕ *(clear/clear glazing and* $\Delta T_{bath} = 10°C$*).*

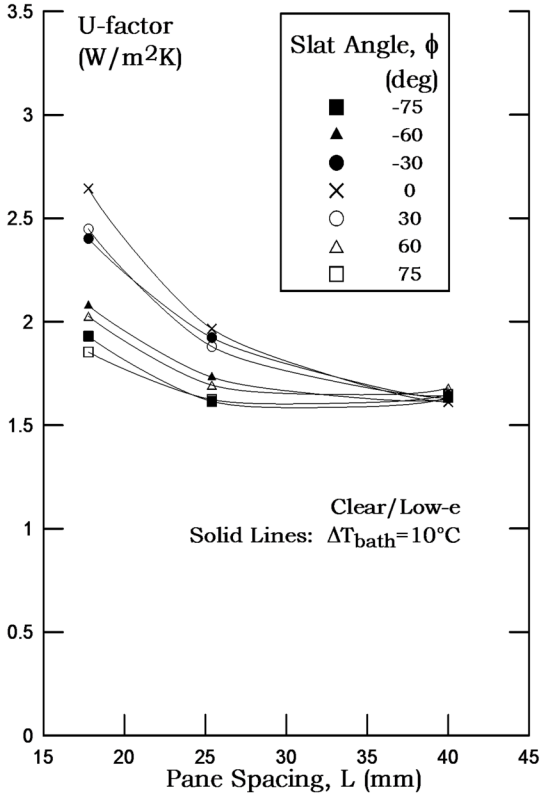

Figure 10 *Measured* U_{cg} *as a function of* L *for various slat angles,* ϕ *(low-e/clear glazing and* $\Delta T_{bath} = 10°C$*).*

Effect of Pane Spacing

Figure 8 shows a clear trend with respect to pane spacing. Although some exceptions are found, when the venetian blind is fully closed or near to being fully closed, U_{cg} decreases as L is increased. This trend is more clearly illustrated by the plots of U_{cg} versus L shown in Figures 9 and 10 for cases without and with a low-e coating, respectively. The data shown in Figures 9 and 10 are from tests done with $\Delta T_{bath} = 10°C$. Similar plots can be generated for U-factors measured with $\Delta T_{bath} = 20°C$.

Recognizing that the radiant heat transfer is unaffected by L, the changes in U_{cg} shown in Figures 9 and 10 must have resulted solely from a change in convective heat transfer.

Figures 9 and 10 also show that a pane spacing of $L = 40$ mm is not large enough for U_{cg} to be independent of L in all cases. When the slat angle is within the range $-30° < \phi < 30°$, U_{cg} is influenced to some extent by changes in L. However, as expected, the influence of L diminishes as L is increased.

CONCLUSIONS

A guarded heater plate apparatus has been used to measure center-glass heat transfer rates through a double-glazed window with a venetian blind in the glazing cavity. Variables examined include pane spacing, temperature difference, slat angle, and the presence of a low-emissivity coating. The measured data have been reported in the form of center-glass U-factor, U_{cg}. Comparison of measured data with earlier measurements and more recent modeling and the high accuracy of the apparatus demonstrated through uncertainty analysis provide confidence in the data produced.

Increased pane spacing results in a noticeable reduction in U-factor. This reduction is most pronounced when the slat angle is small (i.e., blind slats are open or are close to open) and when the pane spacing is small (i.e., marginally larger than the slat width).

The slat angle also has a noticeable effect on U-factor. The maximum U-factor occurs when the blind slats are fully open, all else being equal. This effect is due to the shielding of long-wave radiation by the venetian blind. The influence of slat angle is less pronounced at larger pane spacings.

The presence of a low-e coating reduces the U-factor in all cases.

The effect of temperature difference is small. Only in the case of a very wide pane spacing, an unlikely situation for a commercially produced window, did temperature difference create a noticeable difference in U-factor.

The measurements presented represent a reliable data base for validation of heat transfer models. In addition they provide direct guidance in the development of these models, models that will be able to predict U-factor and solar gain for glazing systems that incorporate enclosed venetian blinds.

ACKNOWLEDGMENTS

This research was supported by Natural Sciences and Engineering Research Council. Golden Windows Ltd. (Kitchener, Ontario) is also acknowledged for supplying key materials used in the assembly of test samples.

REFERENCES

Avedissian, T., and D. Naylor. 2005. Validation of a numerical model of a complex fenestration system. *20th Canadian Congress of Applied Mechanics, Montreal, Quebec*, pp. 242–43.

Carpenter, S. 1992. Thermal performance of window framing systems. *Thermal Performance of the Exterior Envelopes of Buildings, ASHRAE BTECC Conference, Clearwater, Fla.*

ElSherbiny, S.M. 1980. Heat transfer by natural convection across vertical and inclined air layers. PhD thesis, University of Waterloo, Waterloo, Ontario.

ElSherbiny, S.M., G.D. Raithby, and K.G.T. Hollands. 1982. Heat transfer by natural convection across vertical and inclined air layers. *Journal of Heat Transfer* 104:96–102.

Finlayson, E.U., D.K. Arasteh, C. Huizenga, M.D. Rubin, and M.S. Reilly. 1993. WINDOW 4.0: Documentation of calculation procedures. Energy and Environment Division, Lawrence Berkeley Laboratory, Berkeley, California.

Garnet, J.M. 1999. Thermal performance of windows with inter-pane venetian blinds. MASc thesis, University of Waterloo, Waterloo, Ontario.

Garnet, J.M., R.A. Fraser, H.F. Sullivan, and J.L. Wright. 1995. Effect of internal venetian blind on window center-glass U-values. *Proceedings of the Window Innovations Conference, Toronto, June*, pp. 273–79.

Hollands, K.G.T., J.L. Wright, and C.G. Granqvist. 2001. *Solar Energy—The State of the Art—ISES Position Papers*, chapter 2, Glazings and coatings, pp. 29–50. London: James & James Ltd.

Hollands, K.G.T., and J.L. Wright. 1983. Heat loss coefficients and effective $\alpha\tau$ products for flat plate collectors with diathermanous covers. *Solar Energy* 30(3):211–16.

Huang, Y.T. 2005. Thermal performance of double glazed windows with inter-pane venetian blinds. MASc thesis, University of Waterloo, Waterloo, Ontario.

Hum, J.E.Y, K.G.T. Hollands, and J.L. Wright. 2004. Analytical model for the thermal conductance of double-compound honeycomb transparent insulation, with validation. *Solar Energy* 76(1-3):85–91.

Moffat, R.J. 1985. Using uncertainty analysis in the planning of an experiment. *Journal of Fluids Engineering* 107:173–78.

Omega. 2004. *The Temperature Handbook and Encyclopedia*, 5th ed. Stamford, CT: Omega Engineering, Inc.

Rasiah, J. 2003. The design and calibration of a thermopile for the guarded heater plate apparatus. UW 1A Electrical Engineering Work Report, University of Waterloo, Waterloo, Ontario.

Rubin, M. 1982. Calculating heat transfer through windows. *Energy Research* 6:341–49.

Rubin, M., D. Arasteh, and J. Hartmann,. 1987. A correlation between normal and hemispheric emissivity for coated window materials. *International Communications in Heat and Mass Transfer* 14:561–65.

Tasnim, S.H. 2005. Numerical analysis of convective heat transfer for horizontal, between-the-panes louvered blinds. MASc thesis, Mechanical Engineering, University of Waterloo, Waterloo, ON, Canada.

Wheeler, A.J., and A.R. Ganji. 1996. *Introduction to Engineering Experimentation*. Upper Saddle River, NJ: Pearson Prentice Hall.

Wright, J.L. 1980. Free Convection in inclined air layers constrained by a V-corrugated Teflon film. MASc thesis, Mechanical Engineering Department, The University of Waterloo, Waterloo, ON, Canada.

Wright, J.L. 1998. Calculating center-glass performance indices of windows. *ASHRAE Transactions* 104(1):1230–41.

Wright, J.L., and H.F. Sullivan. 1987. Simulation and measurement of windows with low-emissivity coatings used in conjunction with Teflon inner glazings. *ISES Solar World Congress, Hamburg, West Germany*, Vol. 4, pp. 3136–40.

Wright, J.L., and H.F. Sullivan. 1988. Glazing system U-value measurement using a guarded heater plate apparatus. *ASHRAE Transactions* 94(2):1325–37.

Wright, J.L., and H.F. Sullivan. 1989. Thermal resistance measurement of glazing system edge-seals and seal materials using a guarded heater plate apparatus. *ASHRAE Transactions* 95(2):766–71.

Wright, J.L., and H.F. Sullivan. 1994. A two-dimensional numerical model for natural convection in a vertical, rectangular window cavity. *ASHRAE Transactions* 100(2):1193–1206.

Wright, J.L., and H.F. Sullivan. 1995. A two-dimensional numerical model for glazing system thermal analysis. *ASHRAE Transactions* 101(1):819–31.

Yahoda, D.S. 2002. Methods for estimating the effective longwave and solar optical properties of a venetian blind layer for use in centre-glass glazing analysis. MASc thesis, University of Waterloo, Waterloo, Ontario, Canada.

Yahoda, D.S., and J.L. Wright. 2004a. Methods for calculating the effective longwave radiative properties of a venetian blind layer. *ASHRAE Transactions* 110(1):463–73.

Yahoda, D.S., and J.L. Wright, J.L. 2004b. Heat transfer analysis of a between-panes venetian blind using effective longwave radiative properties.*ASHRAE Transactions* 110(1):455–462.

DISCUSSION

Euyatar Erell, Doctor, Ben Gurion University, Israel: Theoretical calculations show that nonvertical (tilted) glazing may give better seasonal performance than vertical glass. Were any of your measurements carried out in a tilted apparatus? How do you think a tilt angle may affect airflow in a glazing system with internal venetian blinds?

John L. Wright: All of the measurements were done with a venetian blind in a vertical glazing cavity. I haven't given any thought to what might happen in a sloped cavity, so it is difficult for me to speculate. I expect that little will change if the slope is near vertical, but the thermal resistance will decrease if the slope is larger. Remember that solar gain is the primary concern when shading systems are being examined, and a small change in this thermal resistance will have little impact on solar gain—only through its influence on inward flowing fraction.